THE JOURNAL OF BIOLOGICAL CHEMISTRY
Vol. 278, No. 32, Issue of August 8, pp. 29609–29618, 2003
Printed in U.S.A.

The Number of Repeat Sequences in Microtubule-associated Protein 4 Affects the Microtubule Surface Properties*

Received for publication, March 3, 2003, and in revised form, May 21, 2003
Published, JBC Papers in Press, May 28, 2003, DOI 10.1074/jbc.M302186200

Kiyotaka Tokuraku‡§, Kazuyuki Matsushima¶, Takanori Matui¶, Hiroyuki Nakagawa¶, Miho Katsuki‖, Rie Majima¶, and Susumu Kotani¶

From the ‡Department of Chemical Science and Engineering, Miyakonojo National College of Technology, 473-1 Yoshio-cho, Miyakonojo, Miyazaki 885-8567, the ¶Department of Biochemical Engineering and Science, Faculty of Computer Science and Systems Engineering, Kyushu Institute of Technology, Fukuoka 820-8502, and the ‖Brain Science Institute, The Institute of Physical and Chemical Research (RIKEN), Wako, Saitama 351-0198, Japan

The microtubule-binding domain of MAP4, a ubiquitous microtubule-associated protein, contains a Repeat region with tandemly organized repeat sequences. In this study, we focused on the variations of the Repeat region, and searched for MAP4 isoforms with diverse Repeat region organizations. We successfully isolated four types of MAP4 cDNAs, which differed from each other in both the number and the arrangement of the repeat sequences, from a single source (bovine adrenal gland). To examine the functional differences among the isoforms, we prepared the microtubule-binding domain polypeptides of three of the four isoforms, and examined their activities. The isoform fragments showed similar degrees of microtubule assembly promoting activity and microtubule binding affinity. This result suggested that the Repeat region variation is not important for the control of microtubule dynamics, which is believed to be the main function of MAPs. On the other hand, the microtubule bundle-forming activity differed among the isoform fragments. The bundle formation was augmented by increasing the number of repeat sequences in the fragments. Based on these results, we propose the hypothesis that the role of the MAP4 isoforms is to regulate the surface charge of microtubules.

In eukaryotic cells, microtubules are essential for various cellular functions, such as mitosis, intracellular transport, and determination of cell shape (1). Several kinds of microtubule-associated proteins (MAPs)[1] have been identified as accessory proteins that can bind to the surface of microtubules. MAPs stimulate tubulin polymerization and stabilize microtubules *in vivo* (1), by assembling tubulin molecules that are otherwise unpolymerizable because of the low subcellular concentration. Therefore, MAPs are believed to play an important role in the regulation of microtubule dynamics in living cells.

Several MAPs (MAP1, MAP2, MAP4, and tau) have been purified from mammalian cells and tissues and characterized well at the biochemical level (2). They are categorized as neural MAPs (MAP1, MAP2, and tau) and non-neural MAPs (MAP4), based on their cellular localization. Studies of the primary structures of MAP1 (3, 4), MAP2 (5–7), MAP4 (8–10), and tau (11–15) have revealed that MAP2, MAP4, and tau are structurally similar, with an N-terminal projection domain and a C-terminal microtubule-binding domain (16–18), whereas that of MAP1 is totally distinct. MAP2, MAP4, and tau have a homologous sequence of 18-amino acid residues responsible for microtubule-binding activity (assembly-promoting (AP) sequence) in the microtubule-binding domain (19–21). Three to five imperfect repeats of the AP sequence have been identified in MAP2 (19), MAP4 (8), and tau (21). Because MAP4 not only distributes ubiquitously (8, 9) but also possesses the structural characteristics common to neural MAPs (MAP2 and tau), analyses of MAP4 will provide clues toward understanding the microtubule-dependent, fundamental cellular processes.

The MAP4 cDNA was originally isolated from Madin-Darby bovine kidney (MDBK) cells (8). Based on the cDNA sequence, the microtubule-binding domain of MAP4 was roughly divided into three subdomains: a region rich in proline and basic residues (Pro-rich region), a region with a tandem organization of AP sequences ("Repeat region"),[2] and a short C-terminal region with hydrophobic and acidic residues ("Tail region"). In the Repeat region, each AP sequence is flanked by interrepeat sequences that are 13–20 amino acids long. This initial report was immediately followed by the isolations of the mouse and human MAP4 cDNAs (9, 10, 22). In human and mouse tissues, MAP4 is encoded by a single gene (9), and the alternative splicing of the MAP4 mRNA gives transcript variants with three to five AP sequences (9, 10, 22). There are still some disagreements on the genetic organizations of the bovine, human, and mouse MAP4 species: No isoform cDNA with an AP sequence organization similar to that of the bovine MAP4 has been detected in human or mouse tissues, whereas bovine MAP4 variants with three or five AP sequences have not been found so far. Therefore, it remains to be determined whether the alternative splicing in the Repeat region is a common characteristic of the expression of mammalian MAP4. In this report, we tried to solve this problem by cloning all of the MAP4 isoforms published at present from the bovine adrenal gland. We previously reported that the bovine adrenal gland is rich in an MAP species with an apparent molecular mass of 190 kDa (23), which turned out to be the bovine MAP4. The abundance

* The costs of publication of this article were defrayed in part by the payment of page charges. This article must therefore be hereby marked "*advertisement*" in accordance with 18 U.S.C. Section 1734 solely to indicate this fact.

The nucleotide sequence(s) reported in this paper has been submitted to the GenBank™/EBI Data Bank with accession number(s) AB079579, AB079580, AB079581, and AB079582 for R5/clone1, R3/clone2, R4α, and R4β, respectively.

§ To whom correspondence should be addressed. Tel.: 81-986-47-1221; Fax: 81-986-47-1231; E-mail: tokuraku@miyakonojo-nct.ac.jp.

[1] The abbreviations used are: MAPs, microtubule-associated proteins; Pro-rich, proline rich; AP sequence, assembly-promoting sequence; MDBK, Madin-Darby bovine kidney; RT, reverse transcription; MES, 2-(*N*-morpholino)ethanesulfonic acid.

[2] Although this region has been referred to as "the AP sequence region" in previous works (27, 38, 41), we used "the Repeat region" in this report, because this term is more commonly used.

of MAP4 in adrenal cells facilitates detailed biochemical analyses (24).

The presence of MAP4 isoforms with different AP sequence organizations suggests that each isoform is assigned to a specific function, depending on the number of AP sequences. In the case of tau, functional differences between the isoforms containing three and four AP sequences were reported (25, 26). Although Chapin *et al.* (22) demonstrated that several different MAP4 isoforms are expressed in different tissues and at various developmental stages, the functional differences of the MAP4 isoforms with three, four, and five repeats have not been elucidated. The tandem organization of the AP sequence had been considered to be important for the nucleation step of tubulin polymerization (20), by allowing a MAP molecule to bind to several unpolymerized tubulin molecules simultaneously. Unfortunately, the experimental results did not support this idea. We have shown that the nucleation activity depends on the Pro-rich region, rather than the Repeat region (27). We (27) and other groups (28) have determined the binding stoichiometry between tubulin and MAPs, which revealed that one MAP molecule with three to five AP sequences can bind to no more than one or two tubulin molecules (27, 28), clearly contradicting the idea that each AP sequence is active in binding to a separate tubulin molecule.

In this study, we successfully isolated all of the MAP4 isoform cDNAs, which have been reported in different species, from a single source. We also investigated how MAP4 modifies its interaction with microtubules by changing the number of AP sequences, using recombinant fragments corresponding to the microtubule-binding domain of bovine MAP4 with three, four, and five AP sequences. This is the first report on the functional differences of MAP4 isoforms *in vitro*.

EXPERIMENTAL PROCEDURES

Materials—Taxol was generously supplied by Dr. N. Lomax, of the Natural Products Branch, NCI, National Institutes of Health, Bethesda, MD. It was dissolved in Me_2SO to a stock concentration of 1 mM and was stored at −20 °C. Restriction enzymes, *Taq* polymerase (Ex *Taq*), RNase-free DNase, and T4 DNA polymerase were purchased from Takara Shuzo Co. Ltd. (Tokyo, Japan). DNA ligase was purchased from Toyobo Co. Ltd. (Osaka, Japan). *Escherichia coli* XL1-blue MRF′ and XL2-blue cells were from Stratagene (La Jolla, CA). The protease-deficient *E. coli* BL-21(DE3)pLysS cells, the protein expression vector pET-21d(+), and the T-Vector pT7Blue were from Novagen (Madison, WI). The AlkPhos-Direct kit, the Hybond N^+ nylon membranes, the AlkPhos direct hybridization buffer, and the ECF detection reagents were from Amersham Biosciences (Tokyo, Japan). The sources of other materials are given in the text. All other chemicals were of reagent grade.

Cloning of MAP4 Isoform cDNAs—MAP4 isoforms were cloned by either reverse transcription (RT)-PCR or cDNA library screening. To carry out RT-PCR, total cellular RNA was isolated from adult bovine adrenal gland (containing the adrenal cortex and the adrenal medulla) by the method of Chomczynski and Sacchi (29). The RNA was treated with RNase-free DNase to remove any contaminating DNA. The DNase-treated RNA was reverse-transcribed with an oligo$(dT)_{18}$ primer pair and recombinant Moloney-murine leukemia virus reverse transcriptase (Invitrogen, Tokyo, Japan). Oligonucleotide primers that would specifically amplify the cDNA encoding the Repeat region of bovine MAP4 were designed based on the previously published *MAP4* sequence (8). The primers, AP-f and AP-r, with the sequences 5′-TGC CAA CGC TTC TGC CC-3′ (nucleotides 2610–2626; numbers indicate positions of primers in the MAP4 cDNA according to the numbering in Aizawa *et al.* (8)) and 5′-GCC CTC AGT CTT CAC GG-3′ (nucleotides 2999–3015), respectively, were purchased from Hokkaido System Science (Sapporo, Japan). These primers spanned a 406-bp portion of the MAP4 cDNA between bases 2610 and 3015. Thirty rounds of amplification were carried out using the following parameters: denaturation at 95 °C for 30 s; annealing at 57 °C for 30 s; and primer extension at 72 °C for 120 s, on an Astec thermocycler (Astec, model PC-700, Fukuoka, Japan). The PCR was completed with a final extension step of 5 min at 72 °C. The resulting PCR products were analyzed by electrophoresis. For cloning PCR products into the T-Vector pT7Blue, the bands encoding the Repeat region of MAP4 were excised from an agarose gel and purified with the QIAquick gel extraction kit (Qiagen, Tokyo, Japan). Purified PCR products were then ligated into the vector. Plasmids from transformed *E. coli* XL2-blue cells were isolated and sequenced.

To construct the cDNA library, total cellular RNA was prepared from bovine adrenal gland, and poly(A+) RNA was purified by oligo(dT)-cellulose column chromatography. The cDNA library was constructed in the λ ZAP II phage vector (Stratagene, La Jolla, CA), and $\sim 2 \times 10^5$ recombinant phages were obtained. To isolate a partial cDNA probe for library screening, the pPA_4 gene (30), encoding the microtubule-binding domain of bovine MAP4, was cleaved with *Pst*I, and a 618-bp fragment was purified by agarose gel electrophoresis. The cDNA probe was labeled with alkaline phosphatase, using the AlkPhos-Direct kit. The cDNA library was plated out at a density of 2×10^4 plaque-forming units/150-mm plate. Plaques were lifted onto Hybond N^+ nylon membranes, and the filters were prehybridized in the AlkPhos direct hybridization buffer containing 5 mM NaCl and 5% blocking agent for 1 h at 55 °C. Hybridization was performed for 16 h at 55 °C in the same solution. Washing and detection with ECF detection reagents were performed according to the manufacturer's protocol. A total of 2×10^5 plaques was screened, and positive plaques were subjected to three successive rounds of purification through plaque isolation and rescreening. The isolated clones were converted *in vivo* to the plasmid form (pBluescriptSK(−)), using the ExAssist/SOLR System (Stratagene). The sequences of all cDNA clones were determined by electrophoresis, using a DSQ-1000 DNA sequencer (Shimadzu, Kyoto, Japan).

Construction of Plasmids for the Bacterial Expression of MAP4 Fragment Polypeptides—To construct the pET-PA_5T plasmid, for the expression of the PA_5T fragment (containing the Pro-rich region, the Repeat region with five AP sequences, and the Tail region), the clone encoding the Repeat region with five AP sequences was first cleaved with *Kpn*I (which cleaves at the unique *Kpn*I site in MAP4 (see Ref. 8 for sequences) and at the *Kpn*I site in the vector portion of the plasmid). The 2.2-kbp *Kpn*I cDNA fragment from the clone was blunt-ended with T4 DNA polymerase and then was cleaved with *Nco*I. The 2.1-kbp *Nco*I/blunt-end cDNA fragment was purified and ligated in-frame into the expression plasmid vector pET21d(+), which had been pretreated with *Bam*HI, T4 DNA polymerase, and *Nco*I. The resultant plasmid, pET-PA_5T, encodes a microtubule-binding domain containing five AP sequences (amino acid residues 579–1098; see Fig. 3*A*). To construct the plasmid pET-PA_3T, for the expression of the PA_3T fragment (containing the Pro-rich region, the Repeat region with three AP sequences, and the Tail region), the same procedure was used, except that a clone encoding the Repeat region with three AP sequences was used instead of the clone encoding that with five AP sequences. The resultant plasmid, pET-PA_3T, encodes a microtubule-binding domain containing three AP sequences (amino acid residues 579–1029; Fig. 3*A*). To construct the plasmid pET-PA_4T, for the expression of the PA_4T fragment (containing the Pro-rich region, the Repeat region with four AP sequences, and the Tail region) with the same strategy, we used the PA_4 gene (30). The resultant plasmid, pET-PA_4T, generates a microtubule-binding domain containing four AP sequences (amino acid residues 579–1072; Fig. 3*A*). None of the plasmids described here encode any additional amino acid residues on either the N- or C-terminal ends. The sequences of these constructs were confirmed as described above.

Purification of Proteins—Microtubule protein was prepared from bovine brains by two cycles of temperature-dependent polymerization/depolymerization (31). Tubulin was purified from the two-cycle microtubule protein fractions by phosphocellulose column chromatography (32), and was stored at −80 °C.

The recombinant plasmids for MAP4 fragments (the pET-PA_3T, pET-PA_4T, and pET-PA_5T plasmids) were each transformed into *E. coli* (BL-21(DE3)pLysS). The expression of these MAP4 fragments was induced by adding isopropyl-1-thio-β-D-galactopyranoside (Takara Shuzo, Tokyo, Japan) to a final concentration of 1 mM in LB medium (10 g/liter NaCl, 10 g/liter bactotryptone, 5 g/liter yeast extract, pH 7.2) containing chloramphenicol (25 μg/ml) and ampicillin (150 μg/ml) at 37 °C. The induction was continued for at least 2 h. The MAP4 fragments were purified from bacterial cells by successive column chromatographies (27). Expression and purification of the PA_4T′ fragment (amino acid residues 534–1072) was carried out according to Aizawa *et al.* (8). Schematic structures of the MAP4 fragments used in this study are shown in Fig. 3*A*.

Protein concentrations were determined in two ways, the conventional Folin-Lowry method (33) and the heated Biuret method of Dorsey (34), using bovine serum albumin as the standard. Because the two methods gave the similar results, concentrations determined by the

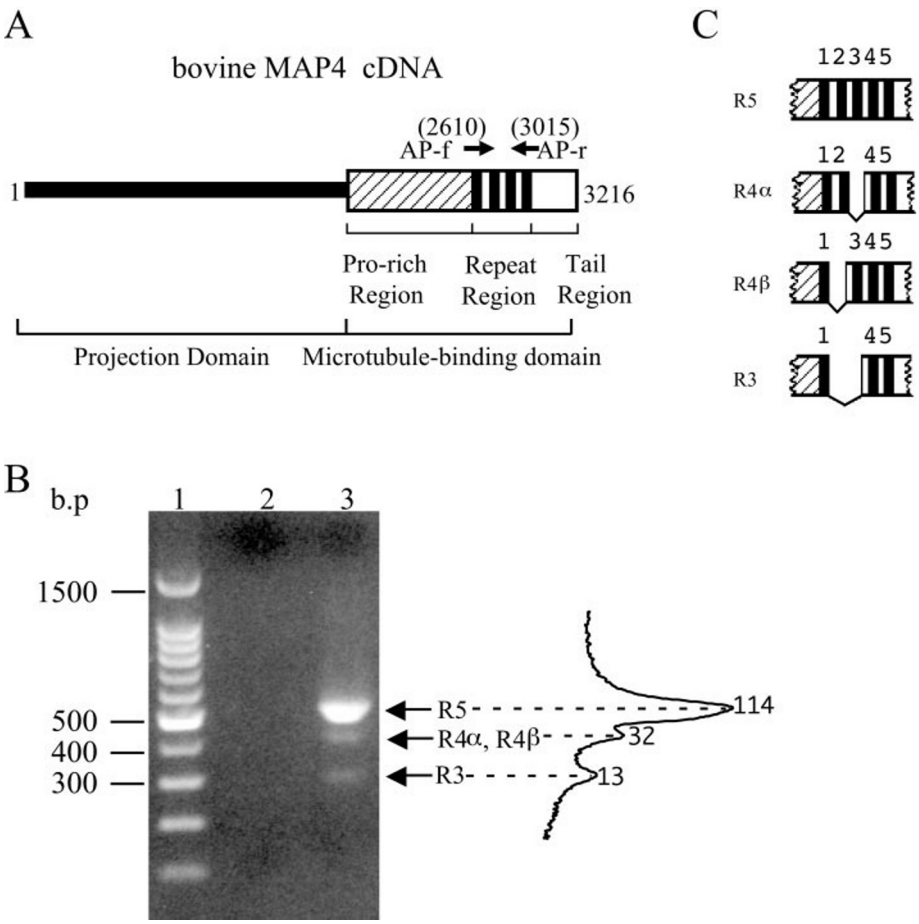

FIG. 1. **Identification of bovine adrenal MAP4 transcripts.** *A*, schematic presentation of the bovine MAP4 cDNA structure (8) and the primers used in this study. A primer set (AP-f and AP-r) was designed to amplify the Repeat region of the MAP4 cDNA. The *arrows* and the *numbers* in *parentheses* indicate the positions of the primers in the MAP4 cDNA sequence, according to the numbering of Aizawa *et al.* (8). *B*, agarose gel electrophoresis of the PCR products. Total RNA prepared from bovine adrenal gland was reverse-transcribed and then amplified with MAP4-specific primers. Molecular weight markers (100-bp DNA Ladder, Takara, Tokyo, Japan) are shown in *lane 1*. *Lane 2* is a control experiment showing the lack of PCR products in the absence of a cDNA template. *Lane 3* shows the PCR products after 30 cycles of amplification. *Arrows* indicate the mobility of the PCR products (R5, R4α, R4β, and R3). The quantities of the three bands in *lane 3* were measured by using Image (National Institutes of Health), with the resultant plot profile and the peak values shown on the *right*. *C*, the Repeat region variation of bovine MAP4 isoforms. The structures of their Repeat regions are schematically presented. Four clones with different AP sequence organizations (R5, R4α, R4β, and R3) were obtained in this study. *Arabic numerals* indicate the number of AP sequences that were renamed in this report.

method of Lowry *et al.* (33) were used. SDS-PAGE was carried out according to Laemmli (35).

Preparation of Antibodies and Immunoblotting—Antiserum against the A_4 fragment (30) was obtained as described previously (36). An antibody specific to the A_4 fragment was purified from the antiserum by membrane affinity adsorption (37). Immunoblotting of the MAP4 fragments was performed as described previously (38). Because the antibody is also reactive to MAP2 and tau, we call it the "anti-(AP sequence) antibody."

Analysis of the Binding of MAP4 Fragments to Taxol-stabilized Microtubules—The analysis of the binding of MAP4 fragments to taxol-stabilized microtubules was performed as described previously (27). Briefly, various concentrations of MAP4 fragments were mixed with tubulin in 100 MEM buffer (100 mM MES (pH 6.8), 0.1 mM EGTA, and 0.5 mM $MgSO_4$) containing 0.5 mM GTP and 30 μM taxol (final volume, 40 μl). The mixtures were incubated at 37 °C and were centrifuged. The pellets were resuspended, and then the supernatants and the pellet solutions were each electrophoresed. The two-dimensional band sizes of the MAP4 fragments and the tubulin on the polyacrylamide gels were measured by an imaging analyzer (scanner: GT9500, Epson, software: Scion Image). The amounts of proteins were determined by comparison with their respective calibration curves, which were prepared in advance by the same method. The Scatchard analysis was performed according to Coffey and Purich (39). The apparent dissociation constant (K_d) and the stoichiometry were calculated from the slope and the intercept, as determined by linear regression (40).

Assay of the Assembly-promoting Activity of MAP4 Fragments under Taxol-free Conditions—Microtubule assembly was monitored by measuring either the amount of polymerized tubulin (sedimentation assay) (27) or the change in absorbance at 350 nm (turbidity assay) (41). The sedimentation assay was done as follows: Various concentrations of MAP4 fragments and tubulin were mixed at 0 °C in 100 MEM buffer containing 0.5 mM GTP. The mixtures were incubated for 30 min at 37 °C and were centrifuged at 28,000 × *g* for 30 min at 37 °C. The pellets were electrophoresed, and the amounts of polymerized tubulin were determined. In the turbidity assay, microtubule assembly was initiated by raising the temperature from 0 °C to 37 °C, and the subsequent polymerization was continuously monitored by the change in absorbance at 350 nm, using a Hitachi U-2000A spectrophotometer (Tokyo, Japan).

Electron Microscopy—Preparations of the microtubule samples for electron microscopic observations were carried out as described previously (27). For negative staining, the sample solutions were mounted on grids, fixed with 2.5% glutaraldehyde in 100 MEM buffer at 37 °C for 5 min, and then stained with 2% uranyl acetate. For thin section observations, sample solutions were centrifuged at 16,000 × *g* for 30 min at 37 °C. The pellets were fixed with 2.5% glutaraldehyde, 3% formaldehyde, and 1% tannic acid in 100 mM cacodylate buffer (pH 7.4) for 1 h at 37 °C, and then were post-fixed with 1% OsO_4 dissolved in the same buffer for 1 h. After dehydration with a graded ethanol series, the pellets were embedded in Poly/Bed 812 mixtures (Polyscience, Inc., Warrington, PA). Ultra-thin sections were cut on a Leica Super Nova ultra-microtome and were stained with 1% uranyl acetate and 0.1% lead citrate. Observations were performed with a JEOL JEM-100S electron microscope (Tokyo, Japan).

RESULTS

Identification and Cloning of MAP4 Microtubule-binding Domain cDNAs—Since we have successfully established a purification system for milligram quantities of MAP4 from bovine adrenal cortex (24), we chose the bovine adrenal gland (containing both the adrenal cortex and medulla) for the source of *MAP4* genes in this study. We first amplified cDNAs encoding the MAP4 Repeat region by an RT-PCR technique (Fig. 1*A*). The MAP4-specific primers were designed so we could obtain PCR products from any possible isoform that covers the Repeat region. If a transcript encoding the original bovine MAP4 (8) was amplified, then the size of the product would be 406 bp. As shown in Fig. 1*B*, we clearly detected a major band of ~500 bp, along with two minor bands of ~400 and 300 bp (*lane 3*). No amplification products were detected in the control sample (*lane 2*). Quantification of the three bands by using Image software (National Institutes of Health) revealed that the ratio

FIG. 2. **Amino acid sequences of the Repeat region and the Tail region of bovine MAP4 isoforms.** Deduced amino acid sequences of clone 1, clone 2, R5, R4α, R4β, and R3 are shown. Amino acid number *861* corresponds to position 861 of the previously reported bovine isoform (8). Amino acids in the *dotted regions* were not determined in this study, because the primer set was designed to amplify the sequence between amino acids 872 and 1036. The newly identified 31-amino acid residues are shown in *boldface*. The five imperfect AP sequence repeats are *underlined*. *Dashes* indicate regions where amino acids are missing as compared with the sequence of R5/clone 1. The stop codon is indicated by an *asterisk*. Note that the last two residues for clones 1 and 2 were *S* and *I*, which are different from the previously reported sequence (SKWLGLA (8)). The nucleotide sequences of the R5/clone 1, R4α, R4β, and R3/clone 2 are available under the DDBJ/EMBL/GenBank™ data bank accession numbers AB079579, AB079581, AB079582, and AB079580, respectively.

of the band sizes of 500, 400, and 300 bp was 7:2:1. The data indicated that at least three cDNA variants exist that encode the MAP4 Repeat region. Unexpectedly, the band of ~400 bp, which would correspond to the clone reported by Aizawa *et al.* (8), was not amplified well. When the RNA samples prepared from the adrenal medulla and cortex were separately subjected to the PCR experiment, no difference was observed between the patterns of PCR products of the two (data not shown). We used the RNA samples prepared from the whole adrenal gland in the subsequent experiments.

We then subcloned and sequenced the three bands. Subcloning of the most efficiently amplified band (~500 bp) revealed that this is a novel bovine MAP4 clone, which encodes a Repeat region with an insertion of 31-amino acid residues between the second and third AP sequences of the known bovine MAP4 clone (8). This 31-amino acid insertion contained an additional AP sequence. We named this new isoform R5 and designated the new AP sequence as the third AP sequence (Fig. 1*C*). Accordingly, the former third and fourth AP sequences were renamed as the fourth and fifth AP sequences in the following text, respectively. Two different subcloned plasmids were isolated from the 400-bp band, although the band in Fig. 1*B* was apparently single. Sequencing analyses revealed one clone to be identical to the original MAP4 isoform (8) with four AP sequences. The other clone also encoded an isoform with four AP sequences, but the arrangement of the AP sequences was different: It contained the third AP sequence instead of the second. We named the former R4α, and the latter R4β (Fig. 1*C*). Four independent clones were obtained from the 400-bp band; two of the clones were R4α, whereas the other two were R4β (data not shown). The ~300-bp band in Fig. 1*B* encoded a clone with a shorter Repeat region (Fig. 1*C*). This clone, named R3, lacked 69 amino acid residues encoding the second and third AP sequences of R5. The results were reproducible, because separate experiments with RNA samples prepared from two independent adrenals gave the same results (data not shown). It is now evident from the data that at least four types of MAP4 isoforms, R3, R4α, R4β, and R5, exist in the bovine adrenal gland. The most abundant form is possibly R5 (~70%).

A comparison of the amino acid sequences of the bovine MAP4 isoforms with those of the human and mouse MAP4 isoforms (9, 22) revealed that R5, R4β, and R3 of bovine MAP4 correspond to the previously reported 5-repeat, 4-repeat, and 3-repeat forms, respectively. The newly identified 31-amino acid sequence of bovine MAP4 completely matched the corresponding 31-amino acid sequence of the human MAP4 (residues 992–1022 (9)), and was similar (more than 90% identity) to that of the mouse MAP4 (residues 965–955 (9)). The similarity was not so surprising, because the Repeat region is highly conserved in all three MAP4 subspecies (9). The Repeat region organizations of the R4β and R3 forms of bovine MAP4 are identical to those of the corresponding human or mouse isoforms.

We then constructed a cDNA library from bovine adrenal gland mRNA, and screened the library for MAP4 isoform clones using a fragment of the R4α cDNA as a probe. Eleven independent positive clones of MAP4 (numbered consecutively from clone 1 to clone 11) were obtained (data not shown). We found that all of the clones, except clone 2, encoded a partial sequence of R5, and that clone 2 encoded a partial sequence of R3. The sequences of the obtained clones, along with those of R3, R4α, R4β, and R5, are shown in Fig. 2. The abundance of the clones encoding the R5 sequence was consistent with the RT-PCR experiment results (Fig. 1*B*), in that the PCR product corresponding to the R5 Repeat region was mainly detected (~70%). Clones encoding R4α or R4β were not obtained, suggesting that the expression levels of the isoforms with four AP sequences are relatively low.

We also noted that the C-terminal sequence of our clones differed from that of the previously reported bovine MAP4 clone (SI instead of SKWLGLA (8)). Because some of the human and mouse MAP4 isoforms also contain SI residues at

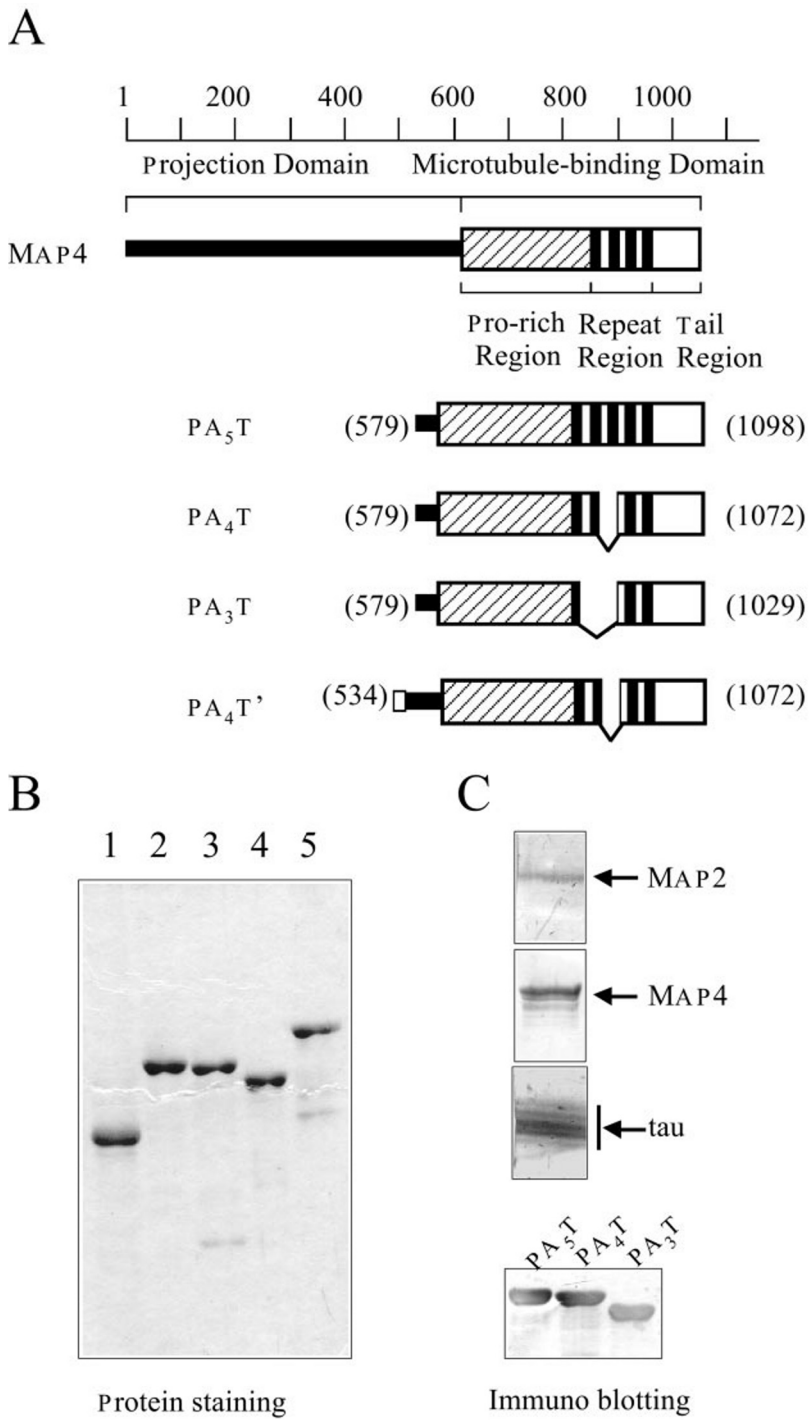

FIG. 3. **Schematic structures of the MAP4 fragment polypeptides used in this study and their representative SDS-PAGE patterns.** *A*, schematic structures of bovine MAP4 (residues 1–1072, according to the numbering in Aizawa *et al.* (8)), the PA_5T fragment (residues 579–1098), the PA_4T fragment (residues 579–1072), the PA_3T fragment (residues 579–1029), and the PA_4T' fragment (residues 534–1072). The *ruler* at the *top* represents the amino acid residue numbers. The projection domain is indicated by *filled thin boxes*. The Pro-rich region is indicated by a *hatched thick box*. The AP sequences (18 amino acid residues) in the Repeat region are indicated by *filled thick boxes*. The Tail region is indicated by an *open thick box*. The additional sequence of the PA_4T' fragment, derived from lacZ′ of pUC (30), is indicated by an *open thin box*. The N- and C-terminal amino acid residue numbers of the fragments are indicated on both sides of each fragment. *B*, SDS-PAGE of purified proteins. *Lane 1*, tubulin purified from two-cycled microtubules; *lane 2*, the PA_5T fragment; *lane 3*, the PA_4T fragment; *lane 4*, the PA_3T fragment; *lane 5*, the PA_4T' fragment. The proteins were electrophoresed on a 10% polyacrylamide gel, and the gel was stained with Coomassie Brilliant Blue R-250. *C*, immunoreactivity of the isoform fragments with the anti-(AP sequence) antibody. The antibody reacted with three MAPs possessing homologous AP sequences (MAP2, MAP4, and tau, *upper three panels*). For efficient transfer onto the membranes, MAP2, MAP4, and tau were electrophoresed separately on 4.5%, 7.5%, and 12.5% polyacrylamide gels, respectively. Then they were transferred to membranes and immunostained with the antibody. The *lowermost panel* shows the immunoreactivity of the PA_5T, PA_4T, and PA_3T fragments with the same antibody. Three micrograms of each of the PA_5T, PA_4T, and PA_3T fragments were electrophoresed on a 10% polyacrylamide gel, transferred, and stained with the antibody.

their C termini, it is possible that the originally reported clone (with the C-terminal sequence of SKWLGLA (8)) is a minor variant. The significance of the C-terminal variation should be assessed in future work. No other mutations were detected in the microtubule-binding domains of R5 or R3, as compared with the known bovine MAP4 sequence. Full-length MAP4 cDNA clones were not obtained, which possibly resulted from the low content of cDNAs encompassing the entire MAP4 coding region in our library. Consequently, the N-terminal portions of R5 and R3 were not characterized.

Expression and Purification of MAP4 Isoform Fragment Polypeptides—To study the functional differences among the MAP4 isoforms with different Repeat region organizations, we constructed expression plasmids for the PA_5T, PA_4T, and PA_3T fragments (containing the microtubule-binding domains of R5, R4α, and R3, respectively). Schematic primary structures of the MAP4 fragments are illustrated in Fig. 3*A*. Expression plasmids containing the R4β microtubule binding domain were not prepared, because we could not obtain a cDNA encoding the entire microtubule-binding domain of the R4β isoform. As we describe in the following section, the dissociation constant and the assembly-promoting activity of the MAP4 isoform fragments (the PA_3T, PA_4T, and PA_5T fragments) were not significantly different from each other. Consequently, it is highly probable that the *in vitro* properties of R4β are similar to those of R4α.

The fragments were purified to near homogeneity (Fig. 3*B*). We also constructed and purified another MAP4 fragment, which contains as additional 54-amino acid residues on the N-terminal end of the PA_4T fragment (this fragment was

TABLE I
K_d of MAP4 fragments to taxol-stabilized microtubules
The dissociation constant K_d (μM) was calculated from the Scatchard plot (data not shown) by the method of Scatchard (40).

	Fragment name						
	PA_3T		PA_4T		PA_5T		PA_4T'
	μM						
Tubulin concentration	5	15	5	15	5	15	15
K_d	0.42	0.44	0.39	0.35	0.27	0.24	0.20

termed the PA_4T' fragment) (Fig. 3*B*, *lane 5*). Our anti-(AP sequence) antibody was reactive to MAP4, MAP2, and tau (Fig. 3*C*, *upper panels*), suggesting that this antibody recognizes the AP sequence. Because the marked difference in the molecular masses of the three MAPs would severely affect their transfer efficiency, the immunoreactivity of the antibody with the three MAPs could not be quantified. When the PA_5T, PA_4T, and PA_3T fragments were immunoblotted with the anti-(AP sequence) antibody, the antibody reacted to the three fragments without any measurable intensity difference (Fig. 3*C*, *lowest panel*). This result suggested that, regardless of the deletion or insertion, the Repeat regions of the three MAP4 isoforms (R5, R4α, and R3) are structurally similar.

Quantitative Analysis of the Interaction between the MAP4 Isoform Fragments and Microtubules—We previously analyzed the binding between taxol-stabilized microtubules and MAP4 fragments (27). Using the same method, we checked whether the number of AP sequences in the Repeat region affected the binding affinity of the fragments to microtubules (Table I). If the AP sequences were all active in binding to microtubules, then the PA_3T, PA_4T, and PA_5T fragments would contain different numbers of microtubule-binding sites from each other. The difference in the K_d values was much smaller than that expected from the difference in the number of binding sites. Although the 2-fold higher binding affinity of the PA_5T fragment over that of the PA_3T fragment may indicate the correlation between the K_d value of the fragment and the number of AP sequences, the same level of increase in the K_d value was also observed when the K_d values of the PA_4T and PA_4T' fragments were compared (Table I). Both fragments have the same four AP sequences, and the PA_4T' fragment has a longer projection domain (Fig. 3*A*). Because the projection domain does not bind to the microtubule directly (30), the data imply that this level of difference in the K_d values can be observed by the structural changes in other parts of the MAP molecule, outside the microtubule binding domain. A longer polypeptide chain probably assumes a more stable conformation in solution, which may indirectly strengthen the interaction between the MAP4 fragment and tubulin. We conclude that the apparent affinities of the fragments depended very little on the number of AP sequences within the fragments.

As described in the introduction, it is now widely accepted that the binding stoichiometry between MAPs and microtubules does not depend on the number of AP sequence repeats. All of the published stoichiometries are about 1 to 2 (tubulin dimers per MAP fragment), even if a MAP has three to five AP sequences (27, 28). As expected, there was no significant difference in the binding stoichiometry among the three fragments (data not shown).

Assembly-promoting Activity of MAP4 Isoform Fragments—To determine whether the number of AP sequences affects the assembly-promoting activity of the fragments, we examined the assembly-promoting activity of the PA_3T, PA_4T, and PA_5T fragments by a sedimentation assay (Fig. 4*A*). The amounts of polymerized tubulin increased with higher concentrations of the added fragments. All three curves were similar, with saturation at 5 μM of each fragment, suggesting that the three MAP4 isoforms (R5, R4α, and R3) possess the same level of assembly-promoting activity *in vitro*. The apparent stoichiometry estimated from Fig. 4*A*, which is about 3:1 (tubulin dimer:MAP fragment), seems contradictory to the binding stoichiometry determined by the Scatchard analysis (27, 28). This discrepancy can be explained as follows: MAPs can stabilize a microtubule even if MAP molecules bind to only a part of tubulin protomers in the assembled microtubule. Actually, maximum polymerization was attained at 5 μM PA_4T' fragment, whereas the fragment continued to bind to taxol stimulated microtubules up to 15 μM (27). Consequently, the apparent stoichiometry estimated from the assembly-promoting activity doesn't correspond to the accurate binding stoichiometry determined by the Scatchard analysis.

The microtubule assembly was also monitored by the change in turbidity at 350 nm (Fig. 4, *B–E*). A comparison of the turbidity values of the three fragments (Fig. 4*E*) revealed a significant difference in turbidity. The sedimentation assay (Fig. 4*A*) indicated that there were no detectable differences in the amounts of microtubule induced by the three fragments, suggesting that the turbidity differences may have resulted from the structural differences among the microtubules induced by the three fragments.

Electron Microscopic Observations of Microtubules Assembled by MAP4 Isoform Fragments—Because the difference in the turbidity of the three samples was most striking at the 5 μM fragment concentration (Fig. 4*E*), the microtubules were allowed to assemble for a short time (0, 30, and 180 s) under the same conditions (5 μM of MAP4 isoform fragments and 15 μM of tubulin) and were observed by negative staining electron microscopy (Fig. 5, *A* and *B*). Short microtubules were observed at the 30-s time point, and the longer incubation (180 s) yielded elongated microtubules (Fig. 5*A*). A further incubation (1800 s) did not affect the appearance of the microtubules (data not shown). The time course of the elongation was consistent with the polymerization process measured by the turbidity (Fig. 4, *B–D*). High magnification views (Fig. 5*B*) revealed that the microtubule structures were normal.

In this electron microscopic observation, the important point to note is the quantitative difference of the microtubule bundles (Fig. 5*A*). The microtubules induced by the PA_3T fragment were rarely bundled, whereas many bundles were observed in the samples of microtubules induced by the PA_4T and PA_5T fragments, with thicker bundles induced by the PA_5T fragment. This indicates that the bundle formation is augmented by increasing the number of AP sequences in the added MAP fragment. To rule out the possibility that the small difference in the binding affinities (Table I) affected the bundle formation, the concentrations of the MAP fragments were increased to 15 μM (Fig. 5*C*). Although this 3-fold increase in the fragment concentration was sufficient to erase the 2-fold decrease in the binding affinity, the results were the same (Fig. 5*C*): no bundles were observed in the 15 μM PA_3T fragment samples, even though the fragment bound to almost all (more than 80%) of the tubulin protomers under these conditions. Therefore, the intrinsic features of each fragment are more likely to be responsible for the bundling efficiency.

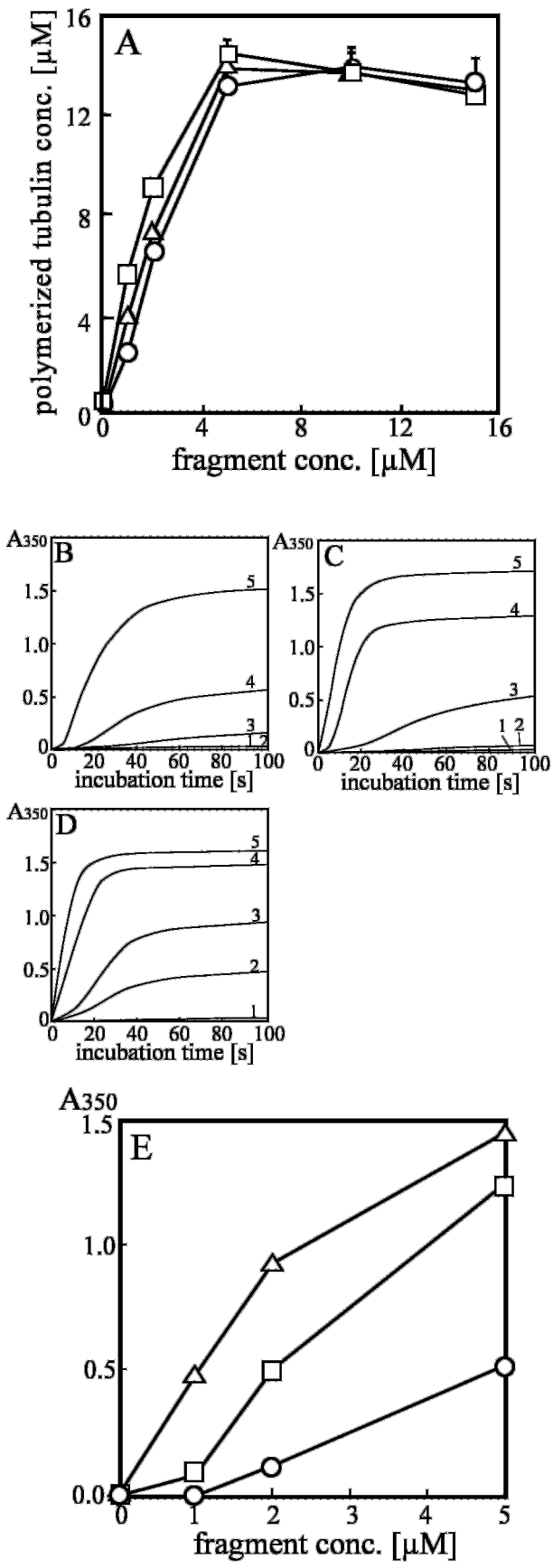

FIG. 4. **The assembly-promoting activity of the MAP4 fragments.** *A*, amounts of assembled microtubules in the presence of the MAP4 fragments, measured by a sedimentation assay. Various concentrations of the MAP4 fragments and 15 μM tubulin were mixed at 0 °C in 100 MEM buffer containing 0.5 mM GTP. The reaction mixtures were incubated at 37 °C for 30 min, and the assembled microtubules were collected by centrifugation. The concentrations of polymerized tubulin were determined as described (27). The amounts of polymerized tubulin are plotted against the concentrations of added PA_3T (○), PA_4T (□), and PA_5T (△) fragments. Averages of three independent experiments are shown. *Error bars* indicate the standard errors. *B–D*, microtubule assembly in the presence of the MAP4 fragments, monitored by the changes in absorbance at 350 nm. *B*, tubulin (15 μM) was mixed with the PA_3T fragment (*curve 1*, 0 μM; *curve 2*, 1 μM; *curve 3*, 2 μM; *curve 4*, 5 μM; *curve 5*, 15 μM). *C*, tubulin (15 μM) was mixed with the PA_4T fragment (*curve 1*, 0 μM; *curve 2*, 1 μM; *curve 3*, 2 μM; *curve 4*, 5 μM; *curve 5*, 15 μM). *D*, tubulin (15 μM) was mixed with the PA_5T fragment (*curve 1*, 0 μM; *curve 2*, 1 μM; *curve 3*, 2 μM; *curve 4*, 5 μM; *curve 5*, 15 μM). Tubulin polymerization was initiated by raising the temperature from 0 °C to 37 °C. *E*, the turbidities at 30 min in *C* (○), *D* (□), and *E* (△) are plotted against the concentrations of the added MAP4 fragments. 15 μM points were not used in this graph because the turbidities of the 15 μM samples were too high for our spectrophotometer to resolve properly.

To analyze the bundle structures, we prepared thin sections of the microtubule samples (Fig. 6). The concentrations of the fragments were set at 15 μM, so that the surface of the microtubules would be saturated by the fragments. Although the microtubules induced by all of the MAP4 isoform fragments were structurally normal, the distances between neighboring microtubules varied, depending on the co-existing fragments. The microtubules induced by the PA_3T fragment were sparse, and most of the microtubules did not bind to each other (Fig. 6*A*, *PA_3T*). Those induced by the PA_4T fragment formed bundles of two to four microtubules (Fig. 6*A*, *PA_4T*). Many bundles of two to ten microtubules were found in the samples of the microtubules induced by the PA_5T fragment (Fig. 6*A*, *PA_5T*). The observed bundle sizes correlated well with the results of the negatively stained micrographs (Fig. 5). No bridge-like structures that connected two adjacent microtubules were observed.

A detailed examination of the photos in Fig. 6*A* revealed that the topologies of the adjacent microtubules could be classified into four groups (Fig. 6*B*, *top left*): a single microtubule with no neighboring microtubule; one microtubule with only one neighboring microtubule; one microtubule linked to two neighboring microtubules; and one microtubule surrounded by three microtubules. Thus, we counted the number of microtubules bound to one microtubule, and then made histograms (Fig. 6*B*). More than 300 randomly sampled microtubules were counted per histogram. Among the microtubules induced by the PA_3T fragment, 80% of the microtubules were single, and 20% were bound to one microtubule (Fig. 6*B*, *PA_3T*). Less than 1% of the microtubules were bound to two or three microtubules (Fig. 6*B*, *PA_3T*). The percentages were different in the samples containing the PA_4T fragment: 40% of the microtubules did not bind to other microtubules, whereas another 40% had one neighboring microtubule (Fig. 6*B*, *PA_4T*). Moreover, 16% of the microtubules bound to two microtubules, and 3% bound to three (Fig. 6*B*, *PA_4T*). More than 80% of the microtubules induced by the PA_5T fragment bound to one or two microtubules (Fig. 6*B*, *PA_5T*). Ten percent of the microtubules bound to three microtubules, and the rest (less than 10%) had no neighboring microtubules (Fig. 6*B*, *PA_5T*). These results indicated that the number of microtubules binding to one microtubule increases with an increasing number of AP sequences in the MAP4 fragments.

DISCUSSION

In this report, we found that four types of MAP4 isoforms, containing different Repeat region organization, are expressed in the bovine adrenal gland. Although Aizawa *et al.* (8) isolated an R4α-type MAP4 cDNA clone from MDBK cells, Chapin *et al.* (22), who isolated three other types of MAP4 cDNA clones (R3,

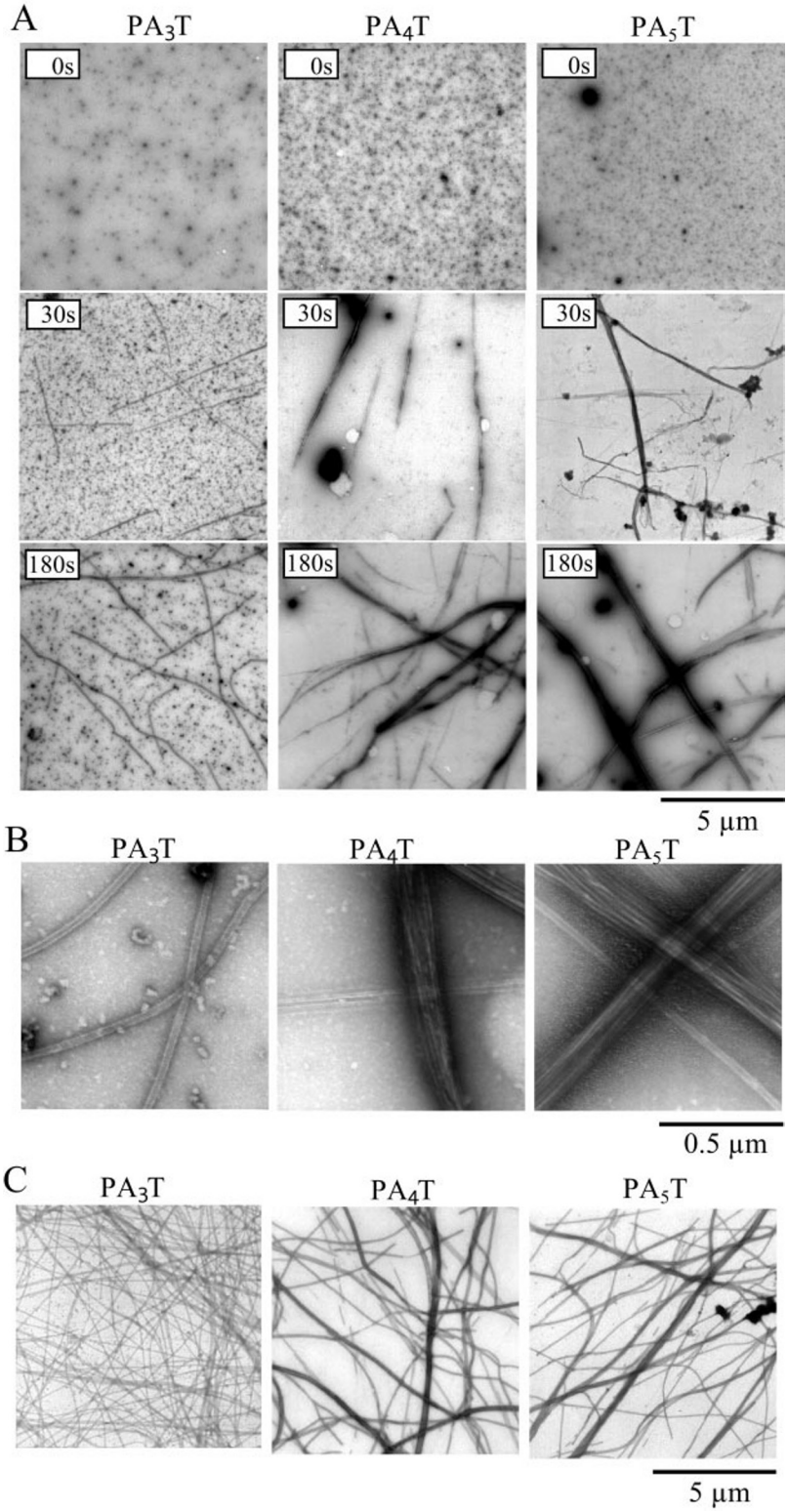

FIG. 5. **Electron microscopic observation of negatively stained microtubules induced by the PA_3T, PA_4T, and PA_5T fragments.** MAP4 isoform fragments and 15 μM tubulin were mixed at 0 °C in 100 MEM buffer containing 0.5 mM GTP. Microtubule assembly was initiated by raising the temperature to 37 °C. *A*, 5 μM MAP4 isoform fragments (the PA_3T, PA_4T, and PA_5T fragments) and tubulin incubated for 0 s, 30 s, and 180 s. *B*, magnified micrographs of microtubules incubated for 180 s in *A*. *C*, 15 μM MAP4 isoform fragments and tubulin incubated for 1800 s.

R4β, and R5) from human or rat, failed to identify the R4α-type, and argued that this is an unusual variant. We demonstrated that all four types of MAP4 cDNA clones (R3, R4α, R4β, and R5, Fig. 1*C*) are expressed in a single source. Chapin *et al.* (22) reported that the expression patterns of these isoforms (R3, R4β, and R5) differ, depending on the cell types and the developmental stages. We also noticed differences in the expression of MAP4 isoforms in the adrenal gland (Fig. 1). Now that the expression of multiple isoforms is clear, their functional differences attract our interest.

Although the AP sequence was originally identified as a specific sequence for MAP binding to microtubules, it is now widely accepted that all of the multiple AP sequences in a MAP molecule are not necessarily active, as we previously discussed (27). In this study, we prepared several microtubule-binding domain fragments of naturally occurring MAP4 isoforms (the PA_5T, PA_4T, and PA_3T fragments) and found that their microtubule assembly-promoting activities were similar, regardless of the number of AP sequences (Fig. 4*A*). This is the first *in vitro* evidence that variations in the Repeat region organization

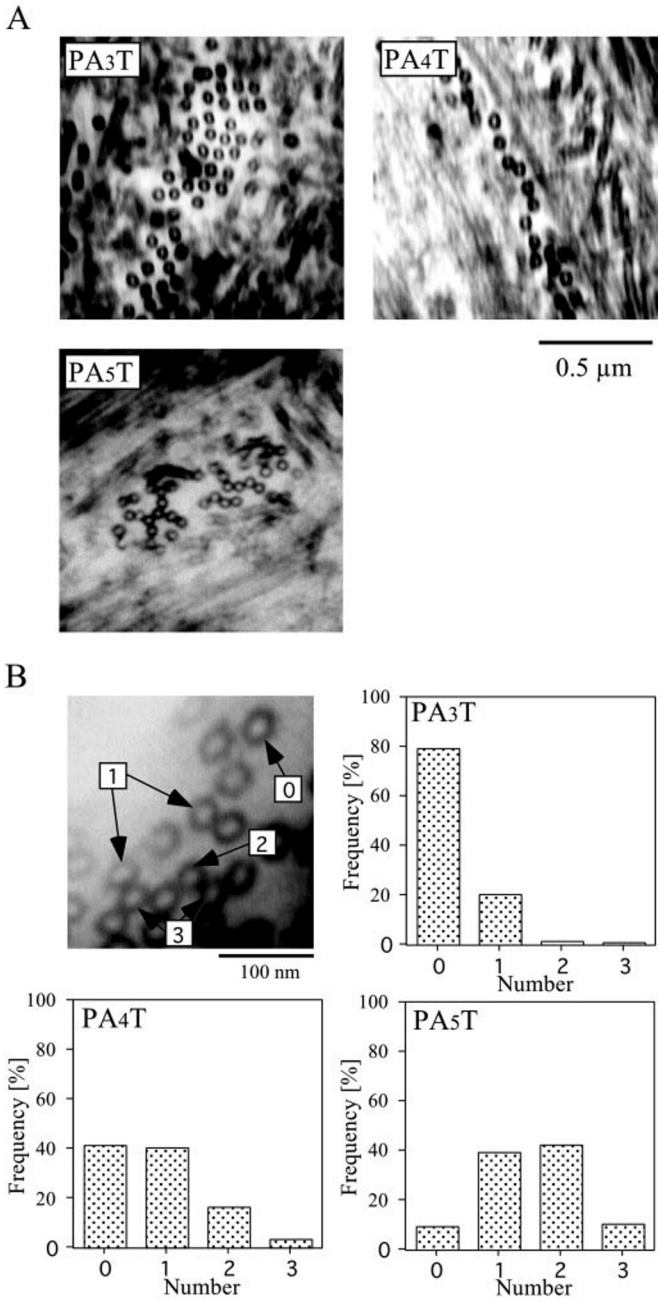

FIG. 6. **Electron microscopic observations of thin sectioned microtubules.** *A*, solutions containing 15 μM of each MAP4 isoform fragment (the PA_3T, PA_4T, and PA_5T fragments) and 15 μM tubulin were incubated for 30 min at 37 °C, and the sample solutions were centrifuged. Thin-sectioned samples were prepared from the pellets. *Scale bar*, 0.5 μm. *B*, analysis of the bundle types in the samples of microtubules induced by MAP fragments. *Above left*, a typical micrograph showing the four types of bundles simultaneously. Microtubules were assembled from 15 μM of the PA_5T fragments and 15 μM tubulin. *Arabic numerals* in the *open boxes* denote the numbers of neighboring microtubules. *Scale bar*, 0.5 μm. Histograms show the frequencies of each bundle type in the microtubules induced by the PA_3T, PA_4T, and PA_5T fragments.

have only minor effects on the assembly-promoting activity. Our results (Fig. 4*A*) suggest that the Repeat region variation is not significant for the control of microtubule dynamics, which are believed to be the main function of MAPs, but is important for other, as yet unknown, functions.

The MAP4 isoform fragments were found to affect the bundling of microtubules (Figs. 5 and 6). What is the role of the fragments in microtubule bundle formation? Electron microscopic observations revealed the following: (*a*) Each fragment induced four types of bundles, with the number of neighboring microtubules ranging from 0 to 3, but the proportion of each type differed depending on the fragments. (*b*) There were no bridge-like structures between neighboring microtubules. Meanwhile, we could not obtain the PA_4T' fragment oligomer using a C-N cross-bridge reagent, 1-ethyl-3-(3-dimethylaminopropyl)carbodiimide (data not shown). The binding stoichiometry between the PA_4T' fragment and the tubulin dimer was ~1 (27). These results refute the hypothesis that a specific MAP-MAP interaction, or a specific tubulin-MAP-tubulin interaction, is responsible for the bundling. We suppose that the bundle formation may be an intrinsic property of microtubules. The neighboring microtubules may bind directly using their surface without any connecting MAP molecules, and the MAP molecules may indirectly regulate the bundling efficiency.

Goode *et al.* (25) reported that tau has a highly flexible and extended conformation in solution. Upon contact with microtubules, the tau structure becomes more ordered. Because MAP4 and tau are structurally similar and compete for microtubule binding (38), the structure of MAP4 may also become ordered when it contacts microtubules. It is possible that the AP sequences are gathered to form a charged region on the surface of the MAP molecule. On the other hand, the MAP4 binding site on the tubulin molecule is estimated to be within the C-terminal region of β-tubulin, including helix 11 (24). The net charge of this region was calculated to be −15, whereas those of the Repeat region of the PA_5T, PA_4T, and PA_3T fragments were +24, +18, and +13, respectively.

On these grounds, we propose a model that explains how the different types of bundles are formed. We suppose that spots, where the acidic charge of the tubulin is neutralized by the basically charged MAP molecule, are produced on the microtubule surface. The neutralization degree would differ, depending on the local basicity of the bound MAPs. The microtubules induced by the PA_3T fragment repel each other, because the fragment cannot neutralize the microtubule surface charge. Consequently, singlet microtubules are most frequently observed, whereas tightly packed bundles are rare. On the other hand, the charge neutralization by the PA_5T fragment is sufficient, so that the maximum bundling (three microtubules around one microtubule) is readily seen, along with some medium-size bundles. The PA_4T fragment induced an intermediate level of bundling, because the basicity of this fragment is the average of the two (the PA_5T and PA_3T fragments).

What physiological functions are shared among the MAP4 isoforms? Iida *et al.* (42) reported that the MTB polypeptide of human MAP4, which corresponds to the PA_5T fragment in this study, induced large bundles of microtubules, but the full-length human MAP4 containing the projection domain did not induce bundles. They proposed that the projection domain has an inhibitory effect on bundling. We also confirmed that MAP4 purified from bovine adrenal cortex, which is largely composed of intact MAP4 molecules containing the projection domain and five AP sequences, does not induce bundles (data not shown). Thus, the bundle formation is not an *in vivo* function of the intact five-repeat molecules, because they usually contain the projection domain. In this report, the functional differences of the isoforms were mainly observed in their effects on microtubule bundling *in vitro*, and we discussed how the modification of the microtubule surface charge might be responsible for the diversity in the bundling patterns. Considering that the MAP4-induced bundling is inhibited by the presence of the projection domain *in vivo*, it may be the variation of the microtubule surface charge itself that is physiologically significant. We propose the hypothesis that the role of the MAP4 isoforms is to

regulate the microtubule surface charge. The interactions between two microtubules, or between microtubules and other microtubule-binding factors (such as microtubule-dependent motor proteins) may be regulated by the microtubule surface charge. Reports on isoform expression can be surveyed from this viewpoint. MAP4 isoforms containing three or four AP sequences are abundantly expressed in the brain, whereas the expression of the five-repeat isoform is restricted to non-neural tissues, such as kidney, spleen, lung, and liver (22). MAP2 and tau, two major neuronal MAPs, have no reported isoforms with five AP sequences (5, 6, 14, 19, 24). There may be a reason why the five-repeat isoforms are not suitable for the neuronal microtubule surface. For example, electrostatic interactions are important for the binding between the basic region of kinesin and the acidic microtubule surface (43–45). It is possible that neuronal microtubule-dependent motors cannot bind to microtubules induced by the MAP4 isoform containing five AP sequences, because of the local basicity of the isoform. Whether the five-repeat isoform interferes with the kinesin motor activity is now being examined.

Acknowledgments—We thank Dr. H. Murofushi for providing the expression plasmid for the PA_4T' fragment, Dr. N. Lomax, of the Natural Products Branch, NCI, National Institutes of Health, Bethesda, MD, for providing the taxol, and M. Nishimura for technical assistance (construction of the cDNA library).

REFERENCES

1. Dustin, P. (1984) *Microtubules*, 2nd Ed., Springer-Verlag, Heidelberg
2. Wiche, G., Oberkanins, C., and Himmler, A. (1991) *Int. Rev. Cytol.* **124,** 217–273
3. Noble, M., Lewis, S. A., and Cowan, N. (1989) *J. Cell Biol.* **109,** 3367–3376
4. Langkopf, A., Hammarback, J. A., Muller, R., Vallee, R. B., and Garner, C. C. (1992) *J. Biol. Chem.* **267,** 16561–16566
5. Lewis, S. A., Wang, D. H., and Cowan, N. J. (1988) *Science* **242,** 936–939
6. Kindler, S., Schulz, B., Goedert, M., and Garner, C. C. (1990) *J. Biol. Chem.* **265,** 19679–19684
7. Kalcheva, N., Albala, J., O'Guin, K., Rubino, H., Garner, C., and Shafit-Zagardo, B. (1995) *Proc. Natl. Acad. Sci. U. S. A.* **92,** 10894–10898
8. Aizawa, H., Emori, Y., Murofushi, H., Kawasaki, H., Sakai, H., and Suzuki, K. (1990) *J. Biol. Chem.* **265,** 13849–13855
9. West, R. R., Tenbarge, K. M., and Olmsted, J. B. (1991) *J. Biol. Chem.* **266,** 21886–21896
10. Chapin, S. J., and Bulinski, J. C. (1991) *J. Cell Sci.* **98,** 27–36
11. Drubin, D. G., Caput, D., and Kirschner, M. W. (1984) *J. Cell Biol.* **98,** 1090–1097
12. Goedert, M., Wischik, C. M., Crowther, R. A., Walker, J. E., and Klug, A. (1988) *Proc. Natl. Acad. Sci. U. S. A.* **85,** 4051–4055
13. Lee, G., Cowan, N., and Kirschner, M. (1988) *Science* **239,** 285–288
14. Himmler, A., Drechsel, D., Kirschner, M. W., and Martin, D. W., Jr. (1989) *Mol. Cell Biol.* **9,** 1381–1388
15. Andreadis, A., Brown, W. M., and Kosik, K. S. (1992) *Biochemistry* **31,** 10626–10633
16. Vallee, R. B., and Borisy, G. G. (1977) *J. Biol. Chem.* **252,** 377–382
17. Aizawa, H., Murofushi, H., Kotani, S., Hisanaga, S., Hirokawa, N., and Sakai, H. (1987) *J. Biol. Chem.* **262,** 3782–3787
18. Aizawa, H., Kawasaki, H., Murofushi, H., Kotani, S., Suzuki, K., and Sakai, H. (1988) *J. Biol. Chem.* **263,** 7703–7707
19. Joly, J. C., Flynn, G., and Purich, D. L. (1989) *J. Cell Biol.* **109,** 2289–2294
20. Aizawa, H., Kawasaki, H., Murofushi, H., Kotani, S., Suzuki, K., and Sakai, H. (1989) *J. Biol. Chem.* **264,** 5885–5890
21. Ennulat, D. J., Liem, R. K., Hashim, G. A., and Shelanski, M. L. (1989) *J. Biol. Chem.* **264,** 5327–5330
22. Chapin, S. J., Lue, C. M., Yu, M. T., and Bulinski, J. C. (1995) *Biochemistry* **34,** 2289–2301
23. Kotani, S., Murofushi, H., Maekawa, S., Sato, C., and Sakai, H. (1986) *Eur. J. Biochem.* **156,** 23–29
24. Tokuraku, K., Katsuki, M., and Kotani, S. (2002) *Rec. Res. Devel. Biochem.* **3,** 315–333
25. Goode, B. L., Chau, M., Denis, P. E., and Feinstein, S. C. (2000) *J. Biol. Chem.* **275,** 38182–38189
26. Utton, M. A., Gibb, G. M., Burdett, I. D. J., Anderton, B. H., and Vandecandelaere, A. (2001) *J. Biol. Chem.* **276,** 34288–34297
27. Tokuraku, K., Katsuki, M., Nakagawa, H., and Kotani, S. (1999) *Eur. J. Biochem.* **259,** 158–166
28. Coffey, R. C., Joly, J. C., Cain, B. D., and Purich, D. L. (1994) *Biochemistry* **33,** 13199–13207
29. Chomczynski, P., and Sacchi, N. (1987) *Anal. Biochem.* **162,** 156–159
30. Aizawa, H., Emori, Y., Mori, A., Murofushi, H., Sakai, H., and Suzuki, K. (1991) *J. Biol. Chem.* **266,** 9841–9846
31. Shelanski, M. L., Gaskin, F., and Cantor, C. R. (1973) *Proc. Natl. Acad. Sci. U. S. A.* **70,** 765–768
32. Weingarten, M. D., Lockwood, A. H., Hwo, S. Y., and Kirschner, M. W. (1975) *Proc. Natl. Acad. Sci. U. S. A.* **72,** 1858–1862
33. Lowry, O. H., Rosebrough, N. J., Farr, A. L., and Randall, R. J. (1951) *J. Biol. Chem.* **193,** 265–275
34. Dorsey, T. E., McDonald, P. W., and Roels, O. A., (1977) *Anal. Biochem.* **78,** 156–164
35. Laemmli, U. K. (1970) *Nature* **277,** 680–685
36. Katsuki, M., Tokuraku, K., Nakagawa, H., and Kotani, S. (2000) *Eur. J. Biochem.* **267,** 7193–7200
37. Terasaki, A. G., Nakagawa, H., Kotani, E., Mori, H., and Ohashi, K. (1995) *J. Cell Sci.* **108,** 857–868
38. Tokuraku, K., Katsuki, M., Matui, M., Kuroya, T., and Kotani, S. (1999) *Eur. J. Biochem.* **264,** 996–1001
39. Coffey, R. L., and Purich, D. L. (1995) *J. Biol. Chem.* **270,** 1035–1040
40. Scatchard, G. (1949) *Ann. N. Y. Acad. Sci.* **51,** 660–672
41. Katsuki, M., Tokuraku, K., Nakagawa, H., Murofushi, H., and Kotani, S. (1997) *FEBS Lett.* **418,** 35–38
42. Iida, J., Itoh, T. J., Hotani, H., Nishiyama, K., Murofushi, H., Bulinski, J. C., and Hisanaga, S. (2002) *J. Mol. Biol.* **320,** 97–106
43. Woehlke, G., Ruby, A. K., Hart, C. L., Ly, B., Hom-Booher, N., and Vale, R. D. (1997) *Cell* **90,** 207–216
44. Okada, Y., and Hirokawa, N. (1999) *Science* **283,** 1152–1157
45. Thorn, K. S., Ubersax, J. A., and Vale, R. D. (2000) *J. Cell Biol.* **151,** 1093–1100